Source-Scaling Validation for Selected Southern California Earthquake Sequences and Application to Ground Motion Prediction

Final Project Report

U.S.G.S Award Number G15AP00001
Kevin Mayeda
University of California, Berkeley, California, 94720
Ph. (510) 328-0466; Fax (510) 643-5811; kmayeda@yahoo.com

Term: December 1, 2014-November 30, 2015

Abstract

The ability to predict the high frequency part of strong ground motions is largely dependent upon the accurate, *a priori* knowledge of the earthquake stress parameter (*e.g*., stress drop scaling). This has direct application to the current SCEC Broad Band Simulation platform as well as Ground Motion Prediction Equations (GMPE's) for PEER, which currently do not use a standard model for the stress drop scaling. However, the behavior of earthquake source scaling has been the topic of significant debate in the earthquake source community mainly because traditional methods require substantial path, site, and source radiation pattern corrections that ultimately yield large variances for corner-frequency estimates and subsequently the stress drop estimates (*e.g.,* see review by *Abercrombie et al*., 2006). Therefore, determining whether or not a magnitude dependence of stress drop exists is often times obscured by large data variance. Alternatively, the coda ratio method by *Mayeda et al*. [2007] is a well vetted technique that has been widely used in the explosion monitoring community for accurate source spectral estimation using sparse station deployments and for use in magnitude, discrimination, and explosion yield estimation, with variances that are typically 3-to-4 times smaller than direct wave methods. The method has been applied to numerous earthquake sequences in a variety of geophysical regions. The coda ratio methodology is similar in every respect to the traditional direct wave spectral ratio methods which takes advantage of co-located earthquakes to remove common path and site effects, the so-called Green's function events. The significant difference however comes from the fact that the coda envelopes are very stable and not sensitive to either the source radiation pattern or source directivity (see *Mayeda and Malagnini*, 2010) and represent a convolution over the entire source process. We present a validation example taken from the M_w 5.9 Wells, Nevada earthquake sequence where we compare 5% damped pseudoacceleration (PSA) ratios with self-similar and non-self similar source scaling. By validating source scaling with PSA ratios, as well as PGA and PGV, these results can be used as in the future as constraints in stress parameterization used in the SCEC's Broad Band Simulation platform.

1) Develop earthquake scaling relationships derived from our coda-based source spectral ratios for 5 earthquake sequences in Southern California
2) Validate scaling relationships using predicted and recorded PSA, PGA and PGV for the Wells, NV sequence which can be used in the future for the other sequences.

Approach

Coda Ratio Processing

Assuming the simple single corner frequency source model [*Aki*, 1967; *Brune*, 1970] the ratio of the moment-rate functions for two events (1 and 2) is given by,

$$\frac{\dot{M}_1(\omega)}{\dot{M}_2(\omega)} = \frac{M_{0_1}\left[1+\left(\omega/\omega_{c_2}\right)^2\right]^{p/2}}{M_{0_2}\left[1+\left(\omega/\omega_{c_1}\right)^2\right]^{p/2}} \qquad (1)$$

where M_0 is the seismic moment and ω_c is the angular corner frequency ($2\pi f_c$) and p is the high frequency decay rate. At the low frequency limit the source ratio shown in equation 1 is proportional to the ratio of the seismic moments $\left[M_{0_1}/M_{0_2}\right]$, whereas at the high frequency limit, equation 1 is asymptotic to $\left[M_{0_1}/M_{0_2}\right]^{\left(1-\frac{p}{3}\right)}$ under self-similarity. If we follow the usual *Brune* [1970] omega-square model and set p=2, the exponent of the high-frequency ratio becomes 1/3. However, it has been proposed by *Kanamori and Rivera* [2004] that the scaling between moment and corner frequency could take on the form,

$$M_o \sim \omega_c^{-(3+\varepsilon)} \qquad (2)$$

where e represents the deviation from self-similarity and is usually thought to be a small positive number. For example, *Walter et al.* [2006] and *Mayeda et al.* [2005] found e to be close to 0.5 for the Hector Mine mainshock and its aftershocks using independent spectral methods. For the current study we use the source spectrum portion of the Magnitude Distance Amplitude Correction (MDAC) methodology of *Walter and Taylor* [2001], which allows for the variation of the corner frequency that does not have to be self-similar. For example,

$$\omega_c = \left(\frac{k\sigma_a}{M_0}\right)^{1/3} \text{ and } \sigma_a = \sigma_a'\left(\frac{M_0}{M_0'}\right)^{\psi} \text{ and } \psi = \frac{\varepsilon}{\varepsilon+3} \qquad (3)$$

where σ_a is the apparent stress [*Wyss*, 1970], σ_a' and M_0' are the apparent stress and seismic moment of the reference event, and ψ is a scaling parameter. For constant apparent stress, ψ = 0 and e =0, however, *Mayeda and Walter* [1996] found ψ=0.25 for moderate to large earthquakes in the western United States. By using the corner frequency defined in (3) into equation 1, we can apply a grid search to find the parameters that best fit the spectral ratio data.

Results

To illustrate the methodology, we turn our attention to local and regional recordings of the M_w 5.9 Wells, Nevada mainshock and 6 aftershocks ranging between M_w ~3.9 and 4.5 (see Yoo and Mayeda, 2013). In this case we considered 11 broadband stations from the

Transportable Array ranging between ~200-230 km at a range of azimuths. All the events have independent regional seismic moment estimates from full waveform inversion by *R. Herrmann* [*pers. comm.,* 2010]. We used 108 narrow frequency bands with central frequencies ranging between 0.03 and 14.19-Hz.

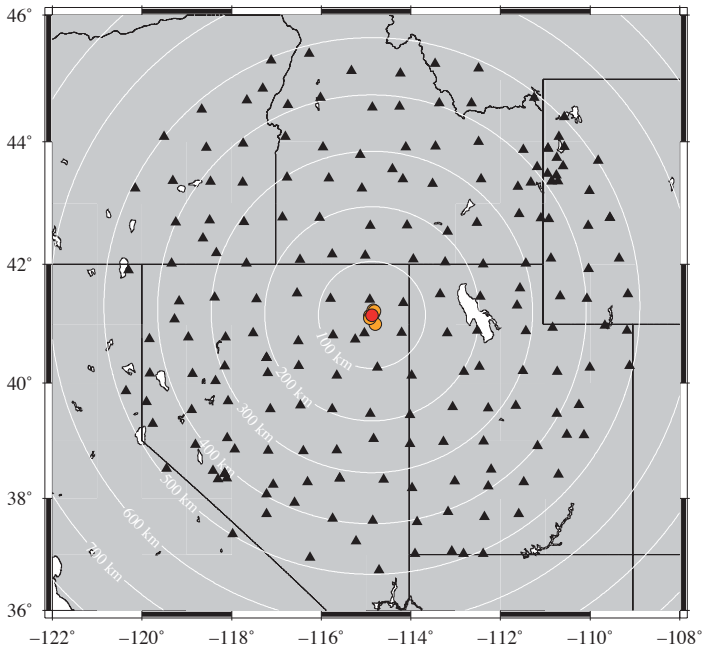

Figure 1. Map of stations used in our study area. Red and orange circles represent locations of the 2008 Wells, NV mainshock and 6 aftershocks, respectively. Black triangles represent 162 broadband stations, most of which were part of the U.S. Transportable Array deployment.

Using all 11 stations, we formed the average spectral ratio between the mainshock and each of the aftershocks, then grid-searched using equation 1 and 3 assuming that the reference moment corresponded to an M_w 5.0 event and the reference apparent stress was varied between 0.5 and 10 bars. As observed for San Francisco Bay Area events, the coda spectral ratios for Wells, Nevada events were very stable, with average standard deviations less than 0.1 for all frequencies. In all cases the high frequency asymptote is significantly above the theoretically predicted value. This is consistent with a break in self-similarity where e is between 0.5 and 1.0, and it is inconsistent with a standard self-similar *Brune* [1970] style omega-square model. What is striking is the low data scatter when compared against results from a conventional direct wave method. These results will be used later to validate peak ground motion which can be used in other data sets such as our results for southern California.

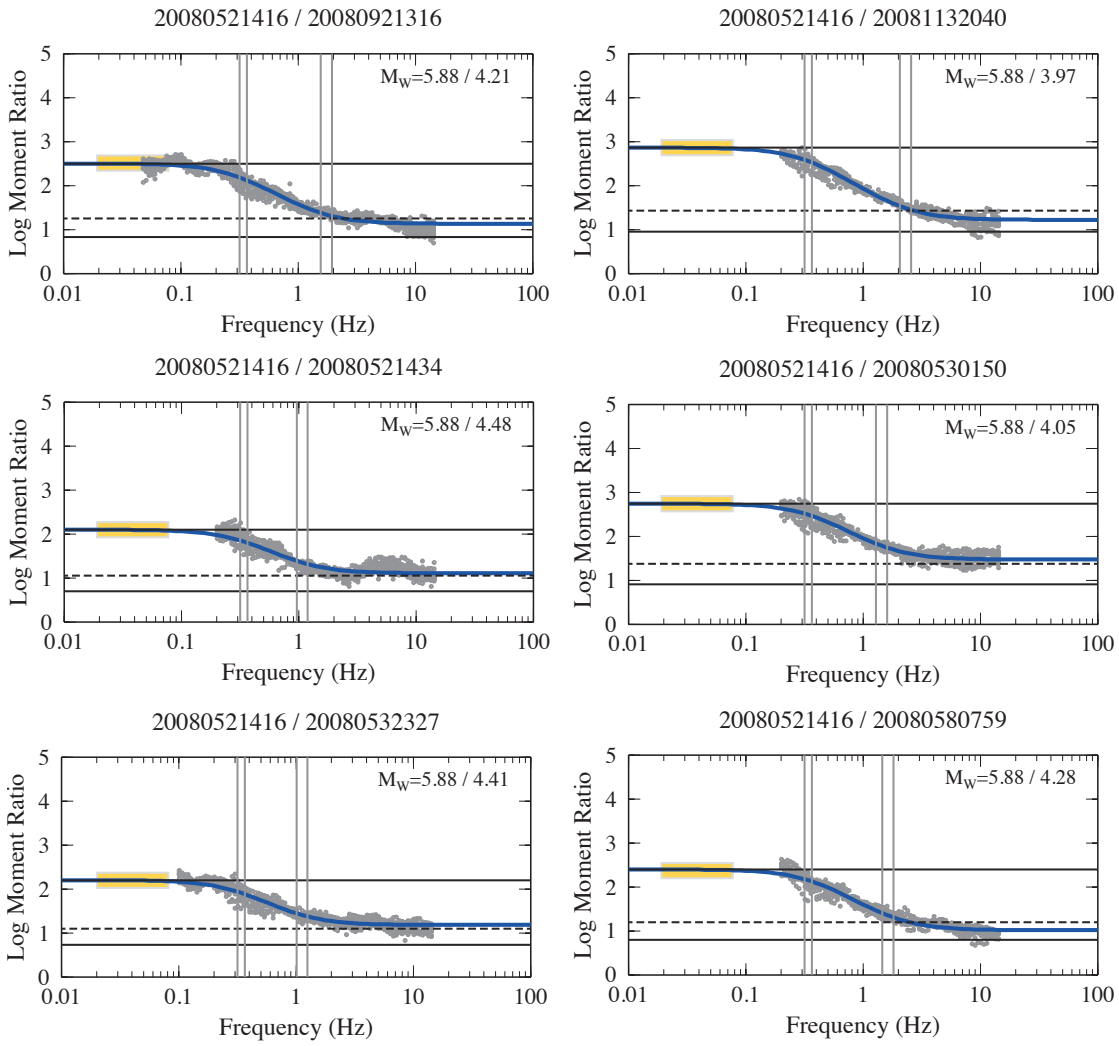

Figure 2. Coda-derived source spectral ratios for the Wells, Nevada mainshock relative to 6 aftershocks are shown as gray points. In each figure, we show the low and high frequency asymptotes from equation 1 as solid black horizontal lines and dashed lines represent the case when p=1.5. Yellow rectangles show regionally-derived seismic moment ratios from *R. Herrmman* (pers. comm., 2010). Blue lines represent the best fitting MDAC spectral ratios that fit all 6 ratios simultaneously. Vertical lines show corner frequency estimates for both the mainshock and aftershocks based upon error analysis.

Southern California Source Scaling

Using the methodology outlined above, we have computed high-resolution coda-derived source spectral ratios using independently derived moment magnitudes from 3-D waveform modeling (as shown in Figure 2) to constrain the long-period ratio levels of the 5 southern California

sequences (Figure 3). Because of ample stations for each sequence we were able to obtain very low variance amplitude ratio estimates.

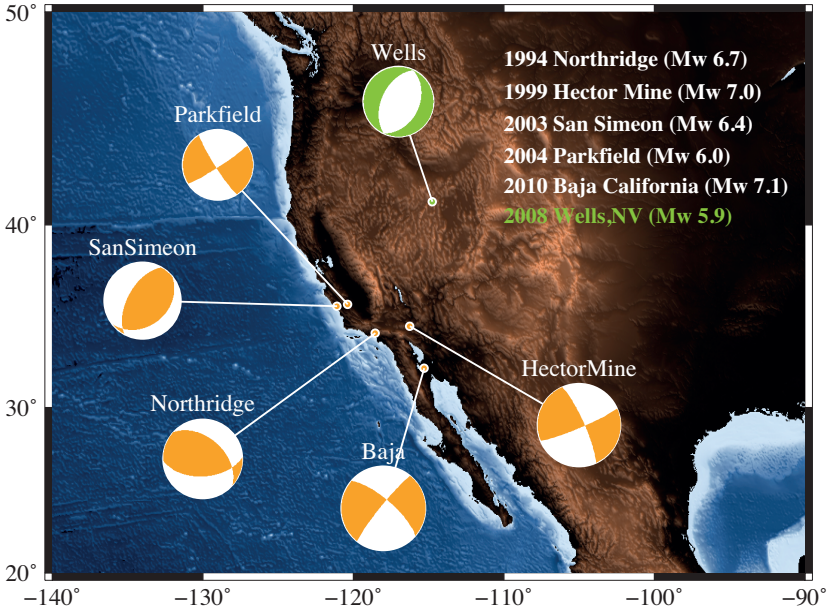

Figure 3. Map showing the 5 southern California mainshocks that we processed as part of our source scaling study as well as the 2008 M_w 5.9 Wells, Nevada earthquake that we will use in our ground motion validation study.

The following Figures 4a-4e show summary corner frequency versus moment scaling for each of the 5 southern California sequences along with error bars. All source parameters are also listed in Table 1 that can be used to constrain future ground motion prediction models.

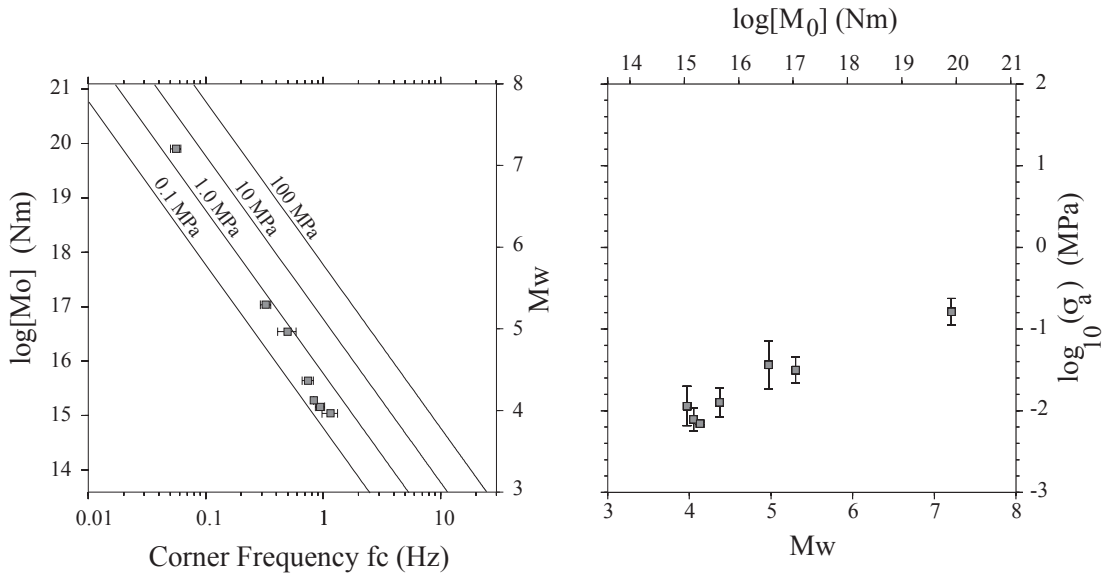

Figure 4a. Baja

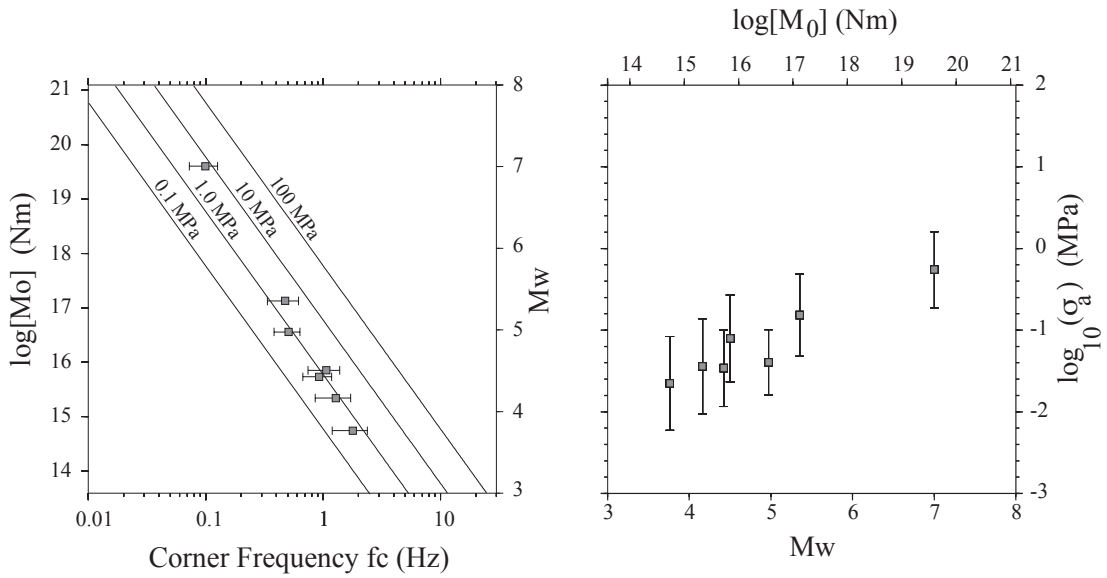

Figure 4b. Hector Mine

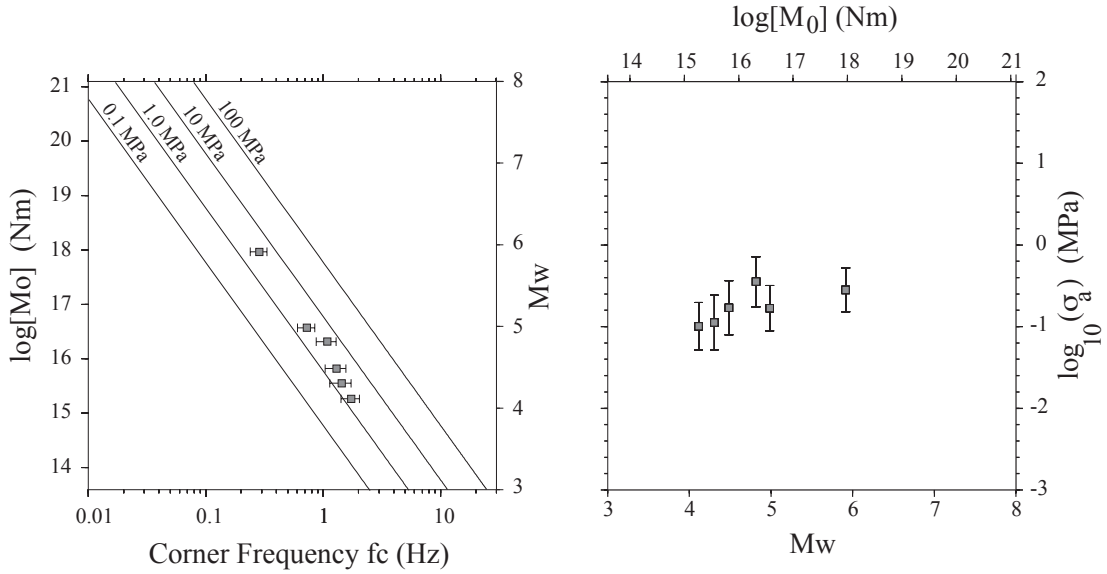

Figure 4c. Parkfield

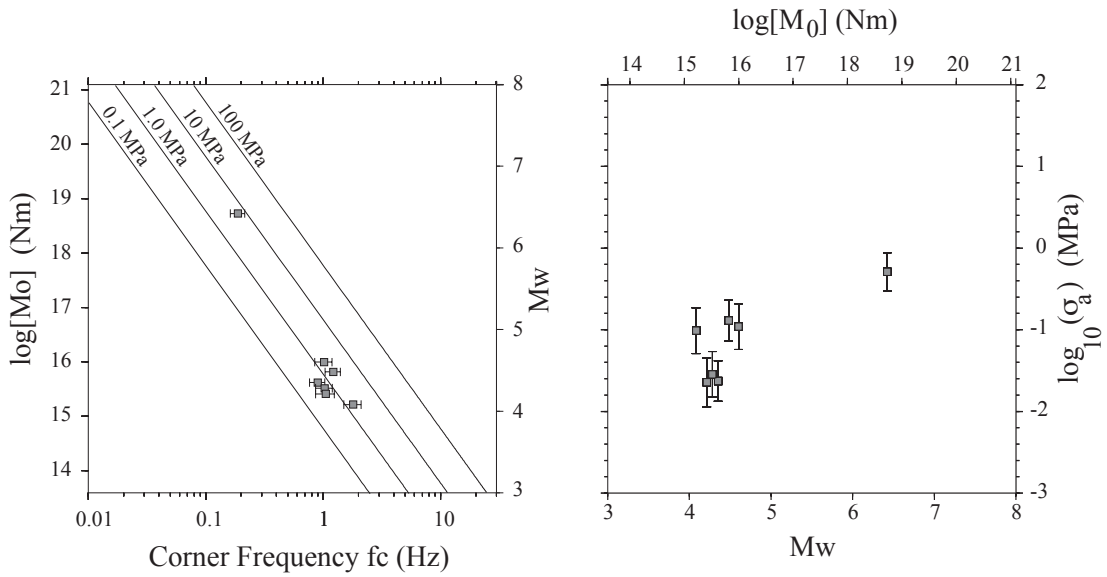

Figure 4d. San Simeon

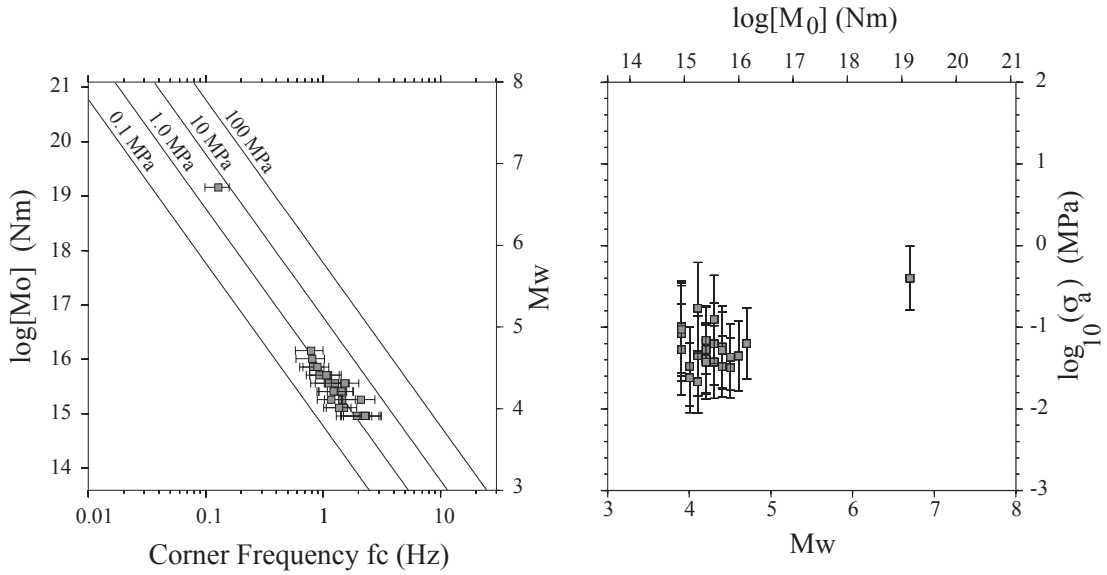

Figure 4e. Northridge

As found with other source scaling studies, including Wells, NV, the stress drop increases with increasing moment, breaking self-similarity. The following provides further evidence that this is affecting direct waves as we study PSA, PGV and PGA.

Validation of Source Scaling Using Peak Ground Motion Data:

Next, we consider Pseudo Spectral Acceleration (PSA) ratios using 162 local and regional stations that surrounded the Wells, NV sequence (Figure1). In Figure 5 we plot 5% damped pseudo-acceleration ratios at 5-Hz between the Wells mainshock and an M_w 4.4 aftershock as a function of azimuth. The median of the data is shown as a solid black line.

Theoretical values from coda-derived source scaling from Figure 6 are shown as the orange line whereas the self-similar prediction is shown as the green line. Black dashed horizontal lines are upper and lower quartiles and gray dashed line represents the theoretical source ratio based upon the two events' focal mechanisms.

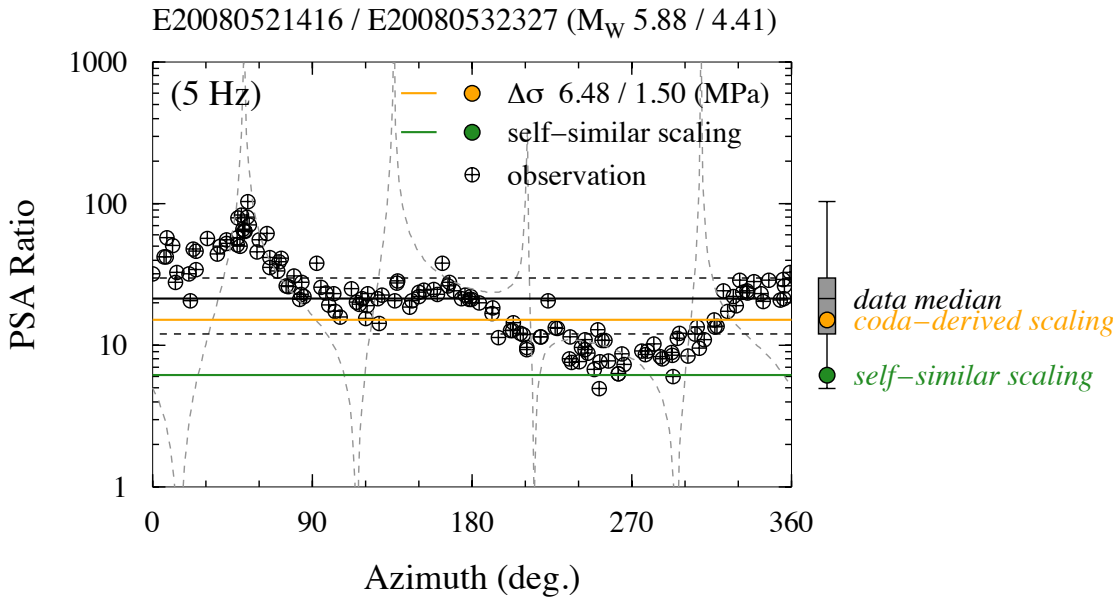

Figure 5. PSA ratio comparison between the mainshock and an aftershock plotted as a function of azimuth. Symbols represent ratio of 5% damped pseudoacceleration ratios at 5-Hz between the Wells, NV mainshock and an M_w 4.4 aftershock. The median of the data is shown as a solid black line. Theoretical values from coda-derived source scaling are shown as the orange line whereas the self-similar prediction is shown as the green line. Black dashed horizontal lines are upper and lower quartiles and gray dashed line represents the theoretical source ratio based upon the two events' focal mechanisms.

We see from Figure 5 that the self-similar assumption falls outside of nearly all the observed data. We note that the observed PSA ratios are free of site response and the variation of larger than a factor of 10 is due to both source radiation pattern and source directivity. In spite of this large variation, the coda-derived estimate (orange line) is very close to the median value of the observed data.

As a further test, we consider PSA ratios taken between the mainshock and six aftershocks for central frequencies ranging between 1 and 10-Hz. Figure 6 shows 'box and whisker' plots of PSA ratios for six mainshock-aftershock pairs. The 50% data range is shown as the vertical gray boxes and the tails represent the full data range. Orange circles show theoretical predictions based upon non-constant source scaling taken from the coda-derived source scaling results, whereas the green circles show the predictions based upon the self-similar assumption. Aside from the results at 1-Hz, it is clear that the self-similar predictions fall well below the observed PSA ratios.

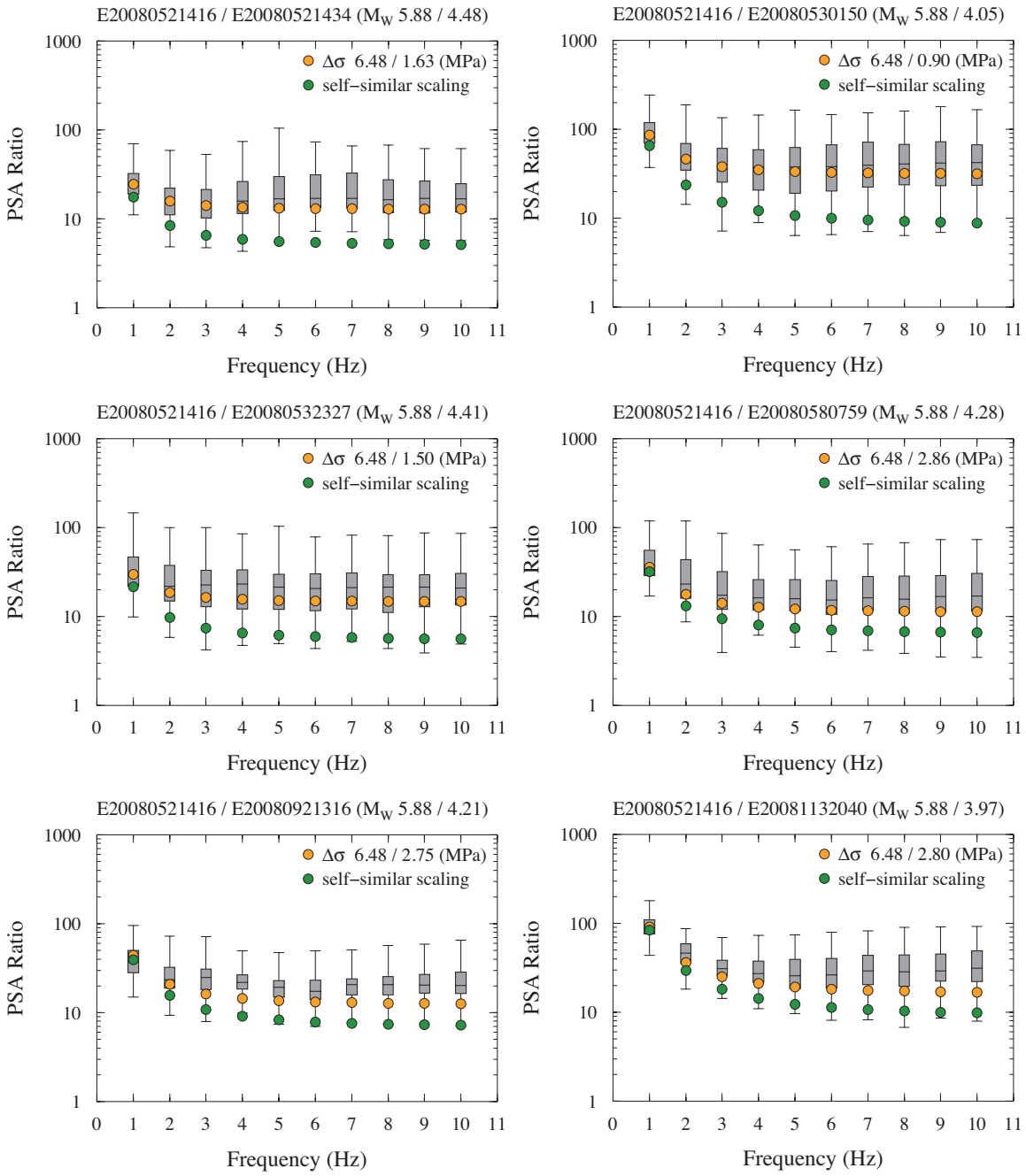

Figure 6. Box and whisker plots of PSA ratios from 1-10-Hz for six mainshock-aftershock pairs. 50% data range is shown in gray box. Orange circles show theoretical predictions based upon non-constant scaling taken from the coda scaling results, and green circles show predictions based on the self-similar assumption which clearly do not match the observed data.

Next, we consider Peak Ground Acceleration (PGA), Peak Ground Velocity (PGV), and Pseudo Spectral Acceleration (PSA) at 1 and 5-Hz of the mainshock. Figure 7 shows our results where blue circles represent the mainshock and yellow circles represent the M_w 4.4 aftershock. Predicted ground motions (blue lines; mainshock, yellow lines; aftershock) are

from the Next Generation Attenuation (NGA) ground motion model by *Campbell and Bozorgnia* (2008). Dotted lines represent ±2 standard deviation of the predicted values. Observed ratios of ground motions of the two earthquakes are about 2-to-3 times larger than those predicted from the NGA ground motion model.

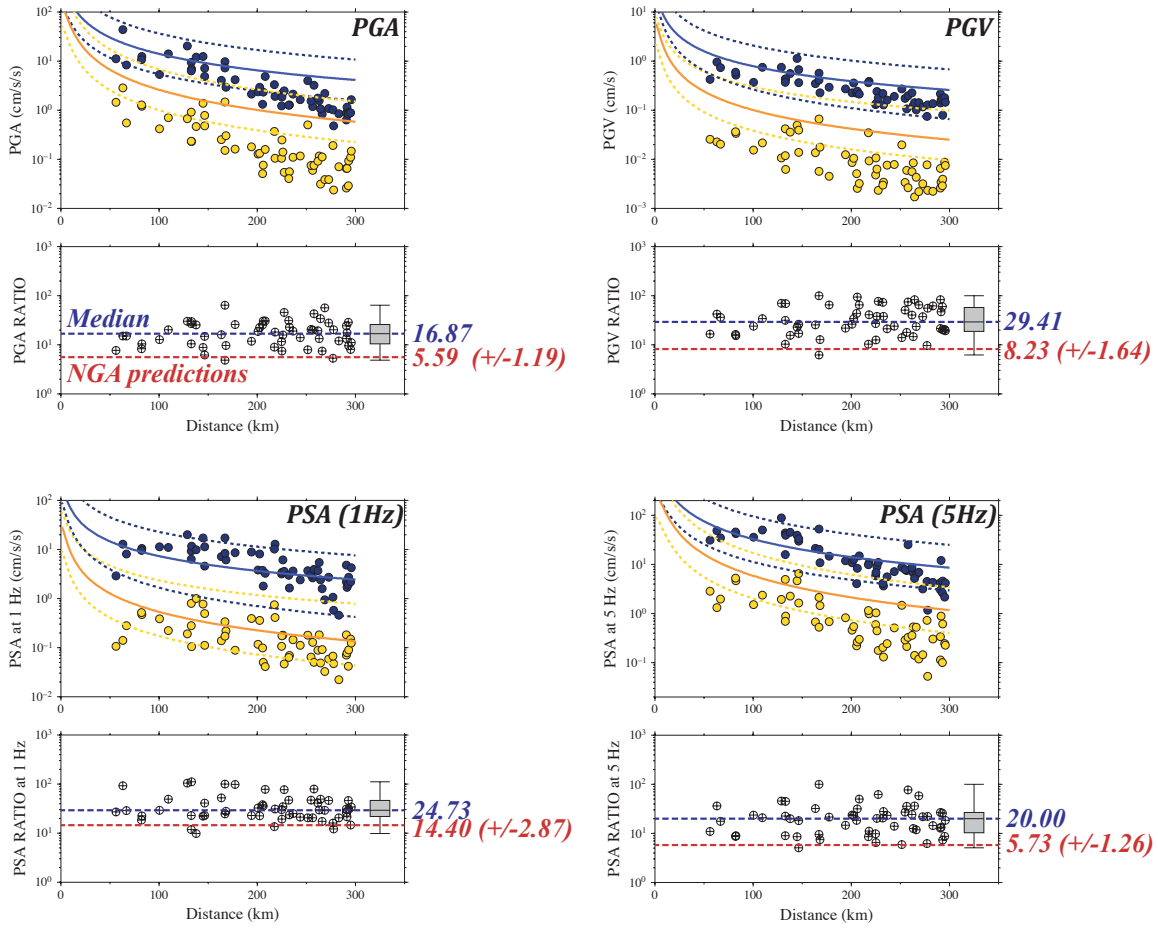

Figure 7. Predicted ground motions (blue lines; mainshock, yellow lines; aftershock) are from the Next Generation Attenuation (NGA) ground motion model by Campbell and Bozorgnia (2008). Dotted lines represent ± 2 standard deviations of the predicted values. Observed ratios of ground motions of the two earthquakes are about 2-to-3 times larger than those predicted from the NGA ground motion model.

Project Summary:

A new high-resolution state-of-the-art methodology using coda envelope ratios has been shown to provide very precise estimates of the average corner frequency, Brune stress drop, and apparent stress using a minimal number of events and stations for 5 southern California earthquake sequences. Table 1 documents ground-truth source spectral parameters derived from this study that can be used as source constraints in future GMPE studies and ground motion simulations in southern California. Furthermore, using the Wells, Nevada sequence, we have demonstrated that NGA predictions of PGA and PSA cannot

simultaneously match moderate and large magnitude events unless source scaling is included (see Figures 5,6,7). Again, the advantages of the coda ratio methodology and its benefits in this study include:

- The coda is not sensitive to lateral variations in structure and effectively homogenizes its energy over a broad area and represents a convolution of the entire source time process.
- Directivity and source radiation pattern will not affect the coda envelope amplitude measurement due to azimuthal averaging.
- Unlike direct wave methods that require large amounts of data to average, the coda method can use a minimal number of events and stations.
- The methodology does not require path and site corrections.
- Clipped direct wave data can still be processed since the coda will be on-scale.

References

Abercrombie, R.E, A. McGarr, G. Di Toro, H. Kanamori, *Earthquakes: Radiated Energy and the Physics of Faulting*, *AGU Geophysical Monograph Series*, *170*, 2006.

Aki, K. (1967), Scaling law of seismic spectrum. *J. Geophys. Res.* 72, 1217-1231.

Brune, J. N. (1970), Tectonic stress and spectra of seismic shear waves from earthquakes, *J. Geophys. Res.* 75, 4997-5009.

Campbell, K. W., and Y. Bozorgnia (2008), NGA ground motion model for the geometric mean horizontal component of PGA, PGV, PGD and 5% damped linear elastic response spectra for periods ranging from 0.01 to 10s, Earthquake Spectra, 24(1), 139-171.

Mayeda, K., and L. Malagnini (2010), Source radiation invariant property of local and near-regional shear-wave coda: Application to source scaling for the Mw 5.9 Wells, Nevada sequence, *Geophys. Res. Lett*. 37, L07306, doi:10.1029/2009GL042148.

Mayeda, K. M. and W. R. Walter, (1996). Moment, energy, stress drop and source spectra of Western U.S. earthquakes from regional coda envelopes, *J. Geophys. Res*., 101, 11,195-11,208.

Mayeda, K., L. Malagnini, W.R. Walter, A new spectral ratio method using narrow band coda envelopes: Evidence for non-self-similarity in the Hector Mine sequence, in press *Geophys. Res. Lett.*, 2007.

Walter, W. R. and S. R. Taylor (2001). A revised magnitude and distance amplitude correction (MDAC2) procedure for regional seismic discriminants: theory and testing at NTS, Lawrence Livermore National Laboratory Report, UCRL-ID-146882, http://www.llnl.gov/tid/lof/documents/pdf/240563.pdf

Walter, W. R., K. Mayeda, R. Gök, A. Hofstetter, The scaling of seismic energy with moment: Simple models compared with observations, *Earthquakes: Radiated Energy and the Physics of Faulting*, *AGU Geophysical Monograph Series*, *170*, 2006.

Wyss, M. (1970), Stress estimates of South American shallow and deep earthquakes, *J. Geophys. Res., 75*, 1529-1544.

Yoo, S.-H., and K. Mayeda (2013), Validation of Non-Self-Similar Source Scaling Using Ground Motions from the 2008 Wells, Nevada, Earthquake Sequence, *Bull. Seismol. Soc. Am*., 103, 2520-2533, doi:10.1785/0120120327.

Table 1. Source parameter information for all 6 earthquake sequences.

Wells

Date	Time	Lat.	Lon.	Depth (Km)	Mw	Strike (°)	Dip (°)	Rake (°)	f_c (Hz)	Δf_c (Hz)	$\log_{10} \sigma_a$ (Pa)	$\Delta (\log_{10} \sigma_a)$
2008/02/21	**14:16:05**	**41.15**	**-114.87**	**11.0**	**5.88**	**25**	**40**	**-90**	**0.3213**	**0.0317**	**6.0661**	**0.1449**
2008/02/21	14:34:00	41.12	-114.89	11.0	4.38	40	60	-65	1.2127	0.1398	5.5437	0.1733
2008/02/22	15:34:00	41.13	-114.91	10.0	3.78	20	40	-80	2.0177	0.2582	5.3042	0.1960
2008/02/22	16:20:00	41.21	-114.86	11.0	3.96	225	55	-55	1.7921	0.2049	5.4227	0.1714
2008/02/22	23:57:00	41.15	-114.93	9.0	4.62	225	35	-40	0.8614	0.0916	5.4597	0.1579
2008/04/01	01:50:00	41.14	-114.92	11.0	3.99	230	55	-60	1.6051	0.2019	5.3217	0.1918
2008/04/22	23:27:00	41.10	-114.92	12.0	4.34	225	40	-85	1.1708	0.1359	5.4377	0.1747
2008/02/27	07:59:00	41.19	-114.83	11.0	4.21	90	85	10	1.6773	0.1976	5.7107	0.1776
2008/02/22	15:10:00	41.16	-114.93	10.0	4.07	250	40	-50	1.4212	0.1684	5.2847	0.1789
2008/04/01	13:16:17	41.23	-114.84	12.0	4.19	85	50	-15	1.5906	0.1865	5.6117	0.1764

Baja California

Date	Time	Lat.	Lon.	Depth (Km)	Mw	Strike (°)	Dip (°)	Rake (°)	f_c (Hz)	Δf_c (Hz)	$\log_{10} \sigma_a$ (Pa)	$\Delta (\log_{10} \sigma_a)$
2010/04/04	**22:40:42**	**32.25**	**-115.29**	**5.0**	**7.10**	**219**	**84**	**-17**	**0.0580**	**0.0071**	**5.6597**	**0.1661**
2010/04/09	05:32:15	32.20	-115.31	5.0	4.03	132	62	-124	0.8599	0.1568	4.5564	0.2631
2010/04/11	16.42:08	32.25	-115.32	5.0	4.63	194	89	-14	0.3819	0.0615	4.4043	0.2207
2010/04/14	22:34:55	32.19	-115.21	5.0	4.17	15	57	-44	0.5992	0.1013	4.2991	0.2374
2010/04/17	16:09:53	32.27	-115.34	11.0	4.23	291	57	-133	0.4859	0.0633	4.1230	0.1786
2010/09/14	10:52:18	32.04	-115.20	8.0	5.03	214	80	-33	0.3617	0.0483	4.9380	0.1813

Hector Mine

Date	Time	Lat.	Lon.	Depth (Km)	Mw	Strike (°)	Dip (°)	Rake (°)	f_c (Hz)	Δf_c (Hz)	$\log_{10} \sigma_a$ (Pa)	$\Delta (\log_{10} \sigma_a)$
1999/10/16	**09:46:44**	**34.59**	**-116.27**	**10.0**	**7.00**	**336**	**80**	**174**	**0.0701**	**0.0219**	**5.7175**	**0.3764**
1999/10/16	12:57:20	34.44	-116.25	5.0	5.32	287	79	25	0.3520	0.1138	5.2970	0.3870
1999/10/16	17:38:48	34.43	-116.25	14.0	4.55	163	75	142	0.6586	0.2384	4.9445	0.4375
1999/10/19	12:20:44	34.71	-116.34	5.0	4.24	178	85	-146	0.7288	0.2761	4.6089	0.4406
1999/10/22	16:08:48	34.86	-116.41	5.0	4.93	267	87	-21	0.3888	0.1535	4.8203	0.4559
1999/10/25	18:26:00	34.62	-116.24	5.0	4.38	144	55	85	0.7003	0.2289	4.7813	0.3952
1999/12/23	14:30:54	34.59	-116.26	10.0	3.74	N/A	N/A	N/A	1.2478	0.5034	4.5485	0.4792

Parkfield

Date	Time	Lat.	Lon.	Depth (Km)	Mw	Strike (°)	Dip (°)	Rake (°)	f_c (Hz)	Δf_c (Hz)	$\log_{10} \sigma_a$ (Pa)	$\Delta (\log_{10} \sigma_a)$
2004/09/28	**17:15:00**	**35.81**	**-120.37**	**8.0**	**5.91**	**57**	**85**	**-7**	**0.2624**	**0.0709**	**5.8114**	**0.3725**
2004/09/29	17:10:00	36.00	-120.54	12.0	5.01	231	90	0	0.6339	0.1765	5.6078	0.3853
2004/11/29	01:54:00	35.94	-120.49	10.4	4.32	323	87	-176	1.2917	0.4205	5.4849	0.4519
2005/05/16	07:24:00	35.93	-120.48	10	4.48	321	88	-170	1.2048	0.3855	5.6353	0.4496
2007/05/22	11:34:00	35.86	-120.41	10	4.15	143	85	-172	1.4410	0.4757	5.3668	0.4827

San Simeon												
Date	**Time**	**Lat.**	**Lon.**	**Depth (Km)**	**Mw**	**Strike (°)**	**Dip (°)**	**Rake (°)**	**f_c (Hz)**	**Δf_c (Hz)**	**$\log_{10} \sigma_a$ (Pa)**	**$\Delta (\log_{10} \sigma_a)$**
2003/12/22	**19:14:00**	**37.75**	**-121.15**	**8.0**	**6.42**	**290**	**58**	**78**	**0.1373**	**0.0272**	**5.7506**	**0.2447**
2003/12/23	03:44:00	35.69	-121.11	5.0	4.35	150	84	-170	0.6562	0.1340	4.6828	0.2522
2003/12/23	05:28:00	35.66	-121.11	5.0	4.28	116	54	91	0.7372	0.1708	4.7235	0.2857
2003/12/23	18:15:00	35.65	-121.05	5.0	4.60	275	47	85	0.7271	0.1719	5.1851	0.2865
2004/01/02	10:45:00	35.68	-121.18	5.0	4.21	327	56	112	0.7412	0.1819	4.6233	0.2954
2004/03/17	23:51:00	35.73	-121.07	5.0	4.48	302	49	91	0.8787	0.1888	5.2561	0.2653
2004/10/02	12:20:00	35.54	-120.81	8.0	4.08	120	48	109	1.2594	0.3059	5.1191	0.2966

Northridge												
Date	**Time**	**Lat.**	**Lon.**	**Depth (Km)**	**Mw**	**Strike (°)**	**Dip (°)**	**Rake (°)**	**f_c (Hz)**	**Δf_c (Hz)**	**$\log_{10} \sigma_a$ (Pa)**	**$\Delta (\log_{10} \sigma_a)$**
1994/01/17	**04:30:55**	**34.24**	**-118.56**	**14.0**	**6.70**	**87**	**53**	**59**	**0.1380**	**0.0307**	**6.1687**	**0.2815**
1994/01/17	13:06:28	34.25	-118.55	N/A	4.60	N/A	N/A	N/A	0.7436	0.1946	5.2021	0.3288
1994/01/17	13:26:45	34.31	-118.45	10.0	4.70	80	58	95	0.7260	0.2069	5.3141	0.3544
1994/01/17	14:14:30	34.33	-118.44	10.6	4.50	267	50	62	0.9602	0.2784	5.3770	0.3599
1994/01/17	15:07:03	34.30	-118.47	11.1	4.20	271	31	58	1.8988	0.5592	5.8119	0.3770
1994/01/17	15:54:00	34.37	-118.62	16.5	4.80	56	44	51	0.7168	0.1911	5.4531	0.3331
1994/01/17	19:35:34	34.31	-118.45	11.7	4.00	299	19	75	2.0764	0.7162	5.6166	0.4068
1994/01/17	22:31:53	34.34	-118.44	12.4	4.10	269	55	71	1.2309	0.3518	5.1007	0.3615
1994/01/19	14:09:14	34.23	-118.50	14.8	4.50	74	72	61	1.0060	0.2856	5.4384	0.3613
1994/01/21	18:39:15	34.30	-118.46	10.6	4.60	116	44	51	0.8055	0.2051	5.3087	0.3183
1994/01/21	18:53:44	34.32	-118.48	10.7	4.30	111	29	60	1.2297	0.3832	5.3926	0.3843
1994/01/24	05:50:24	34.36	-118.63	13.6	4.29	71	72	49	1.1278	0.3189	5.2744	0.3486
1994/01/24	05:54:21	34.37	-118.63	16.4	4.20	84	32	35	1.3096	0.3715	5.3322	0.3593
1994/01/27	17:19:58	34.27	-118.56	13.3	4.40	34	0	-4	1.1504	0.3722	5.4549	0.3810
1994/02/03	16:23:35	34.30	-118.44	9.5	4.09	95	34	93	1.3818	0.3989	5.2361	0.3617
1994/02/06	13:19:27	34.29	-118.48	9.4	4.00	118	59	90	1.7540	0.5720	5.3998	0.4033
1994/05/25	12:56:57	34.31	-118.31	9.4	4.50	88	53	65	0.8379	0.1997	5.2143	0.3010